ANALYSIS OF VISCOUS FLOW OVER SWEPT WINGS

Egon Krause

Aerodynamisches Institut
Rheinisch-Westfälische Technische Hochschule Aachen, Germany

Abstract

Compressible laminar and incompressible laminar and turbulent flows are investigated for three swept wings with infinite aspect ratio at various Reynolds numbers. The predictions obtained by finite-difference integration of the boundary-layer equations are compared with experimental data for a pressure distribution of the NACA Profile 63_1-012 at zero angle of attack and with the NLR measurements on an infinite swept wing. Three closure assumptions have been tested in comparison calculations. Second- and fourth-order accurate solutions show that laminar flows can be calculated without difficulty up to separation. For turbulent flows the closure assumptions fail near separation when large cross flows are present.

1. Introduction

Future design of aircraft will rely more heavily on prediction methods than was possible in the past. Pressure distributions will to a greater extend be determined from direct integration of the Euler equations as skin friction coefficients will be obtained from integration of Prandtl's boundary-layer equations for three-dimensional flows. This is of importance since control of the boundary layer on wings and other wetted surfaces of the airplane can result in substantial drag reduction. However, before such predictions become possible, more powerful methods of analysis than those presently in use will have to be developed. Some of the goals which can be reached in the near future were recently described in [1]. Restricting the consideration to viscous flows over lifting surfaces in particular one can identify two major problem areas where future research should concentrate on. One problem consists in providing a more accurate description of viscous flow effects in optimization procedures for lift and drag; the other problem concerns the control of the boundary layer to such a degree that a large portion of the flow can be maintained laminar. According to [1] a laminar-flow controlled airplane would result in ten to twenty percent lower direct operating costs in comparison to the "turbulent" design.

As far as the optimization problem is concerned the techniques presently used have reached a high degree of perfection. Their major shortcoming is, however, that most of the methods are completely based on potential flow analysis and fully ignore the flow displacement through boundary layers on the whole, not to mention their transition and separation.

Another problem of equal difficulty is the prediction of turbulent boundary layers in three-dimensional flows. In them the mechanism of momentum exchange in three dimensions is not fully understood. Recent research on this subject has brought some improvement of the mathematical techniques of the prediction methods; however, because of lack of experimental data models which describe the momentum exchange in three-dimensions reliably have not been developed so far. Instead, all models presently being used are extensions of those developed for two-dimensional flows, no matter whether integral- [2] or finite-difference techniques [3] are considered. It may therefore be possible to predict small cross-flows, in agreement with experimental data, but in flows with large lateral deviations (Refs. [4] and [5]) the Reynolds stresses need not be the same for the two tangential directions and can therefore not be predicted in this manner. A first attempt to adjust a model for the eddy viscosity to the cross-flow was made in [6]. Therein an observation of Ref. [4] was applied in a calculation to predict the measurements of [5]. No general conclusion can however, be drawn from the results, as for example all other calculations in [6] were carried out with an isotropic eddy viscosity.

An isotropic eddy viscosity was also used in Ref. [7]. Therein Adams computed the boundary layer on a swept wing with infinite aspect ratio as investigated experimentally by Altman and Hayter in Ref. [8].

Attempts have been made (Refs. [9] and [10]) to adapt the law of the wall to three-dimensional flows. These modifications improve in one case (Ref. [9]) the accuracy of the prediction but do not contribute to a more general formulation for the turbulent transport mechanism in the outer part of the boundary layer.

This paper sets out to demonstrate the application of a soluton recently developed for general three-dimensional boundary layers [11], here adapted to infinite-swept conditions. First compressible laminar flows over a wing are analysed downstream from the leading edge. Then the experimental data of [5] and [8] are recalculated with three scalar formulations for the eddy viscosity. In the comparison of the results second- and fourth-order finite-difference approximations are shown to have a noticable effect on the accuracy of the prediction, which could easily be attributed to inadequacies of the physical models adopted.

2. Boundary-Layer Equations for Infinite-Swept Wing Conditions

In the present investigation the surface of the wing is assumed to be flat in a first approximation and all curvature effects are neglected. The governing equations are then valid only for a boundary sheet in which the pressure remains constant in the direction normal to the surface of the wall. Let x, y, z be Cartesian coordinates, x and y being measured normal and parallel to the leading edge in the plane of the wing and z normal to it; the corresponding velocity components are u, v, and w. For an infinite aspect ratio all derivatives in the y-direction vanish identically in the governing equations. The continuity equation may then be written [11] in the following form:

$$\frac{\partial}{\partial x}(\rho u) + \frac{\partial}{\partial z}(\rho w) = 0 \tag{2.1}$$

Because of the parabolic nature of the two momentum equations and the energy equation a vector form combining all three equations can be introduced

$$A_1 \frac{\partial F}{\partial x} + A_2 \frac{\partial F}{\partial z} + A_3 \frac{\partial^2 F}{\partial z^2} + B = 0 \tag{2.2}$$

Although conservative formulation is often preferred, equation (2.2) is given in non-conservative form. At the present time not enough information is available to justify a alternative form of equation (2.2). The quantity F is a column vector with components u, v, and the stagnation enthalpy h_s. The coefficient matrices are defined as follows

$$A_1 = g_1 I, \quad g_1 = \rho u \tag{2.3}$$

where I is the identity matrix of order three. The matrices A_2 and A_3 consist again of a factor and a matrix, which in special cases reduces to the identity matrix. The factors are defined as

$$g_2 = \rho w - \frac{\partial}{\partial z}[\mu(1+\varepsilon_x)] \tag{2.4}$$

$$g_3 = -\mu(1+\varepsilon_x) \tag{2.5}$$

The last two equations allow for an extension of the solution to turbulent flows. The quantity ε_x stands for the ratio of the apparent stresses and the Stokes stresses in the x-direction, and a similar expression ε_y can be defined for the direction parallel to the leading edge.

$$\varepsilon_x = -\overline{\rho u' w'}/\tau_{zx}; \quad \varepsilon_y = -\overline{\rho v' w'}/\tau_{zy} \tag{2.6}$$

For compressible flows, the heat flux due to turbulent transport may be expressed in the same form

$$\kappa = \overline{\rho w' h_s'}/q_z \tag{2.7}$$

With equations (2.4) – (2.7) the matrices A_2 and A_3 can be written as

$$A_2 = g_2 \begin{pmatrix} 1 & 0 & 0 \\ 0 & 1+e_{22} & 0 \\ 0 & 0 & 1+e_{23} \end{pmatrix} \tag{2.8}$$

$$A_3 = g_3 \begin{pmatrix} 1 & 0 & 0 \\ 0 & 1+e_{32} & 0 \\ 0 & 0 & 1+e_{33} \end{pmatrix} \tag{2.9}$$

The excentricities e_{ij} are determined from the difference of the apparent stresses and the ratio of the turbulent and the molecular heat flux coefficient:

$$e_{22} = +\frac{1}{g_2}\frac{\partial}{\partial z}(e_{32} g_3) \tag{2.10}$$

$$e_{23} = \frac{1}{g_2}\frac{\partial}{\partial z}(e_{33} g_3) \tag{2.11}$$

$$e_{32} = +\frac{\mu}{g_3}(\varepsilon_x - \varepsilon_y) \tag{2.12}$$

$$e_{33} = -\frac{\mu}{Pr}\frac{(1+\kappa)}{g_3} - 1 \tag{2.13}$$

The inverse of the negative value of the first term in equation (2.13) is often referred to as turbulent Prandtl number. All excentricities vanish, if ε_x and ε_y are equal and if the turbulent and the molecular Prandtl number are equal to unity. The vector B in equation (2.2) is defined through the pressure gradient and the sum of the rest of the heat flux term and the dissipation function.

$$B = \begin{bmatrix} \frac{\partial p}{\partial x} \\ 0 \\ -\frac{1}{2}\frac{\partial}{\partial z}\left\{g_3\left[e_{33}\left(\frac{\partial u}{\partial z}\right)^2 + (e_{33} - e_{32})\left(\frac{\partial v}{\partial z}\right)^2\right]\right\} \end{bmatrix} \tag{2.14}$$

For the solution of equation (2.2) initial and boundary conditions have to be prescribed. The initial conditions can easily be generated since equation (2.2) reduces to an ordinary differential equation for the stagnation or attachment line at the leading edge. Integration of the resulting equation may be facilitated by finite-difference or Runge-Kutta procedures.

The boundary conditions for equation (2.2) are the usual zero-slip condition at the wall and the outer edge condition:

$$F(x, y, 0) = 0; \quad \lim_{z \to \infty} F = F_e(x, y) \tag{2.15}$$

Aside from the boundary conditions, which can either be provided from potential flow analysis or experiments, closure assumptions must be intro-

duced to define the functions e_{32} and e_{33} if turbulent flows are considered. Despite considerable experimental efforts during recent years little or no information exists, from which expressions can be derived for ε_x and ε_y. The data presented for example, in Ref. [4] are of inadequate accuracy and do not encourage one to attempt a correlation. For this reason, the exchange coefficients ε_x and ε_y will be assumed to be scalars for turbulent flow calculations. This assumption must be considered very critically as the available models are all extensions of those derived for two-dimensional flows. Despite some successful predictions general conclusions cannot be drawn from any of the calculations published so far. Since the limitations of the various models are unknown, three of them will simultaneously be incorporated in the integration for turbulent flows: The following models, which all are based on the scalar assumption $\varepsilon = \varepsilon_x = \varepsilon_y$ were chosen: Michel's version of the mixing length approximation [12], according to which the mixing length l is determined from the equation

$$\frac{l}{\delta} = 0.085 \,\mathrm{th}\left(\frac{K}{0.085}\,\frac{z}{\delta}\right) \qquad (2.16)$$

where K is von Kármán's constant (K = 0.4).
The mixing length l is inserted in the van Driest damping factor

$$F = 1 - \exp\left[-\frac{l}{26K\mu}(\tau\rho)^{1/2}\right], \qquad (2.17)$$

and finally ε results from Prandtl's approximation as

$$\varepsilon = \rho F^2 l^2\left[\left(\frac{\partial u}{\partial z}\right)^2 + \left(\frac{\partial v}{\partial z}\right)^2\right]^{1/2} / \mu \qquad (2.18)$$

Another expression for the mixing length is introduced by Pletcher in [13]. While equation (2.16) defines the mixing length for the entire boundary-layer thickness three different approximations are used in Pletcher's polynomial curve fit of experimental data:

$$\frac{l}{\delta} = K\left[1 - \exp\left(-z^+/26\right)\right](z/\delta);\quad 0 < z/\delta < 0.1 \qquad (2.19)$$

$$\frac{l}{\delta} = K\left[1 - \exp\left(-z^+/26\right)\right](z/\delta)$$
$$- 1.53506\,(z/\delta - 0.1)^2 + 2.75625\,(z/\delta - 0.1)^3$$
$$- 1.88425\,(z/\delta - 0.1)^4;\quad 0.1 < z/\delta < 0.6$$

$$\frac{l}{\delta} = 0.089; \qquad 0.6 < z/\delta$$

$$\varepsilon = \rho l^2\left[\left(\frac{\partial u}{\partial z}\right)^2 + \left(\frac{\partial u}{\partial z}\right)\right]^{1/2} / \mu$$

In the outer portion of the boundary layer l is assumed to be constant. The coordinate z^+ is defined in terms of the friction velocity

$$z^+ = (v^+/\nu)\,z;\quad v^+ = (\tau/\rho)^{1/2} \qquad (2.20)$$

A third modification is presently employed in Ref. [6]. In this approximation ε is given by an inner and outer law of the form

$$\varepsilon_i = \rho K^2\left[1 - \exp(-z^+/26)\right]^2\left[\left(\frac{\partial u}{\partial z}\right)^2 + \left(\frac{\partial v}{\partial z}\right)^2\right]^{1/2} z^2/\mu$$
$$\varepsilon_o = \rho K_1 v_e \delta^* \gamma / \mu \qquad (2.21)$$

In equation (2.21) the friction velocity is adjusted to pressure gradient flows. Equation (2.20) must then also include the pressure gradient in the x-direction. This approximation has been used in Ref. [3]. The displacement thickness δ^* must be evaluated from both velocity components. In Ref. [6] it was recently suggested that the two-dimensional value should be a reasonable approximation also for three-dimensional flows. The effect of this approximation will be demonstrated later in a sample calculation. The value of the constant K_1 is 0.0168 and the intermittancy factor γ is determined from

$$\gamma = \left[1 + 5.5(z/\delta)^6\right]^{-1} \qquad (2.22)$$

The models given in the equations above all represent first-order closure relations. They clearly cannot take into account the variation of the exchange coefficients in the two coordinate directions but represent a mean value. Such a simplification is not justified for flows with strong pressure gradients near separation and all models are expected to fail in the vicinity of the separation point. Before the results obtained from the integration of equation (2.2) are presented the method of integration will briefly be outlined.

3. Comments on the Method of Integration

The integration of equation (2.2) can be facilitated through finite-difference approximations for laminar and turbulent flows. This does not mean, as is frequently claimed, that transition can be predicted. Although several empirically determined transition parameter have recently been evaluated for infinite swept wings [14], the validity and the range of application of these parameters has not been established. For the solution of the governing equations the position of the transition point must therefore be assumed. The finite-difference solution used in the present investigation is an adaption of the solution of Ref. [15] and [16] to infinite swept wing conditions. The major details are described in Ref. [11].

For laminar flows there are, in general, no major difficulties in the integration since all derivatives are, indeed, of order unity and reliable error bounds can be obtained by an order of magnitude analysis of the truncation errors. Although the governing equations are non-linear, local linearisation is preferably employed to construct linear implicit difference equations, which, in general, allow a step size of about one order of magnitude larger than explicit difference equations. Reduc-

tion of equation (2.2) to a first-order system is possible and has been done in Ref. [17]. In the present analysis the original second-order equation is retained since it immediately leads to difference equations which have a tridiagonal matrix structure. The simultaneous solution of the N difference equations can be avoided by employing the well-known recursion relations for such matrices and the construction of an efficient algorithm is rather simple.

It was noted in [11] that in turbulent flows because of large velocity gradients near the wall and because of extremely large gradients of the apparent turbulent viscosity considerable numerical errors may result in the integration. Most of the available integration schemes have an overall error of order two and for acceptable numerical errors the step sizes must be taken rather small. The analysis of the errors is not simple as they arise from different sources. The major error sources are: The order of the truncation error, the magnitude of the three step sizes Δx, Δy, and Δz; the error for the iteration process for the normal velocity component; the error with which the outer edge conditions are approximated; the accuracy of the finite-difference approximation of first- and second-order derivatives of the velocity components at the wall. At the present time the step sizes can only be chosen according to experience. This does not impose difficulties for laminar flows, although a method which enables the determination of the proper step size would be most desirable. In the same way error bounds for the iteration process and the outer edge condition are difficult to estimate. The error bound for the outer edge conditions may cause significant changes in the magnitude of the maximum value of the apparent viscosity [16]. Thereby a substantial falsification of all flow quantities obtained through the integration procedure chosen may result. This purely numerical error can easily be attributed to the model adopted for the turbulent shear stresses and may lead to wrong conclusions.

It is often believed that by telescoping the grid, the accuracy of the solution can be improved. This conclusion is only correct if the problem contains one dependent variable so that the location of the extrema of the function and of the higher-order derivatives can be located. Then by adjusting the step size, a consistent accuracy or overall error may be obtained. This approach can not be recommended when the problem contains more than one dependent variables as for example in turbulent boundary layers. The gradient of the tangential velocity components attain their maximum values at the surface while the apparent viscosity approaches its maximum somewhere in the boundary layer; the gradient $\partial\mu / \partial z$ can be very large on both sides of the maximum so that telescoping the grid near the wall (because of the large velocity gradients) would even enlarge the truncation errors in the field. Another example can be given for compressible boundary layers. For constant wall temperatures, the static temperature reaches its maximum value, again, some distance away from the wall. For high Mach-numbers the gradients tend to be steep, which in turn may cause large higer order derivatives. Again, telescoping near the wall and stretching the grid near the outer edge will not improve the accuracy of the solution. In [11] a simple method was tested successfully to overcome the difficulties just described. The three components of equation (2.2) are divided by g_3 so that in equation (2.10) and (2.11) the derivatives of g_3 with respect to z can be replaced by the derivatives of the logarithms. The evaluation of $\ln g_3$ increases the calculation time per grid point, but the accuracy is considerably improved as was shown in Ref. [11]: In a sample calculation the error remained almost constant while the number of grid points was reduced by a factor of eight. The corresponding step sizes were $\Delta z = 0.025$ and 0.2.

Another means of improving the accuracy of the solution consists in reducing the overall truncation error from second to fourth order. This can be done with relatively little effort for the direction normal to the wall as was shown in [18]. By using Taylor-series representation for the first and second-order derivatives, three-point finite-difference equations of fourth order can be obtained. The overall increase of program statements is about ten percent. Although the algorithm can be constructed - as for the second-order solution - with three net points, it must be pointed out that the calculation of the coefficients g_2 requires five net points. The reduction of the truncation error has been a valuable tool in testing the numerical accuracy of the solution, since it can be evaluated with the recursion relations of the second-order solution; by comparing the latter with the former the effect of numerical errors can be studied, as will be shown later. Such an analysis is of particular interest for turbulent flows.

The last point to be mentioned concerns the evaluation of the shearing stress at the wall. Several investigations rely on an evaluation of τ_w which is based on three to five grid points. If the net spacing is sufficiently small, such end-point formulas may be justified. In turbulent flows, particularly for large net spacings a better approximation for τ_w may be derived, if it is assumed that the shearing stress is constant for the first step of integration at the wall. An improvement of as much as twenty percent has been observed in test calculations [11]. This assumption actually is in consistent with the development of fourth-order finite-difference representation, but may be replaced by consistently employing the compatibility conditions at the wall to the required degree of accuracy. Further details of the solution may be found in Ref. [11]. Although fully three-dimensional

flows require a more complicated program logic, extension of the solution for equation (2.2) is straight forward. However, as was pointed out in [19] stable solutionscan only be obtained if the Courant-Friedrichs-Levy condition is satisfied for the subcharacteristics, which for three-dimensional boundary layers are given by the projections of the stream-lines on planes parallel to the surface. In the next section some flow field analysis of viscous flows over infinite swept wings, as obtained in the present investigation, will be described.

4. Boundary-Layer Predictions for Infinite Swept Wing Conditions

Several boundary-layer flows over swept wings of infinite aspect ratio have been analysed with the method of solution described in the preceeding sections. For the first example the following flow conditions were chosen. A laminar boundary layer in a free-stream with Mach numbers $M_\infty = 0.649$, 0.749 and 1.298and a Reynolds number of approximately $3 \cdot 10^6$. The sweep angle φ of the wing was assumed to be zero for the first Mach number, 30° for the second, and 60° for the third. The pressure distribution was determined experimentally for the upper surface of the wing in [20]. In all three cases considered supersonic flow exists and extends over 20 percent of the chord, where a shock can be identified. The pressure coefficient is depicted in the upper part of Fig. 1.

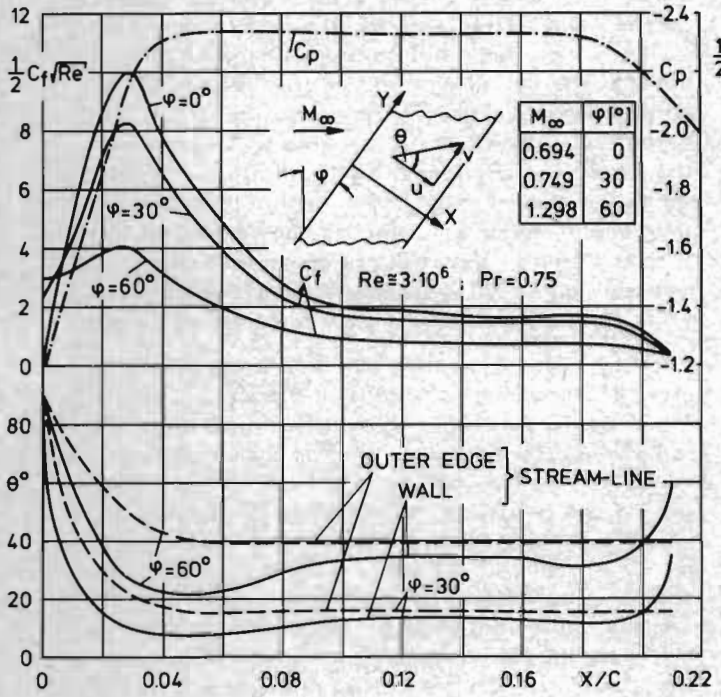

Fig. 1: Pressure-, skin-friction coefficient and flow turning angle in a laminar compressible boundary layer on the upper surface of a swept wing with infinite aspect ratio.

The boundary layer characteristics were determined by an adapted version of the solution for fully three-dimensional flows of [21]. The modification of the solution was carried out by Dr. E. H. Hirschel of the DFVLR-Institut für Angewandte Gasdynamik. He also provided the data shown in Fig. 1. The skin-friction coefficient as obtained from this solution (Fig. 1) attains a maximum a short distance downstream from the stagnation line. It is noted that for $\varphi = 0^\circ$ the maximum is about two and on half times higher than for $\varphi = 60^\circ$. Separation is observed at about 20 percent of the chord. Considerable flow deflection in the boundary layer takes place near the maximum of the shearing stress. For $\varphi = 60^\circ$, the direction of the limiting stream-lines near the wall deviates by some 20° from that of the external flow(lower part of Fig. 1).

The second flow is an incompressible one which was investigated experimentally by Altman and Hayter [8] already in 1951 and more recently by Adams [7], who developed a second-order finite-difference solution for infinite-swept wing conditions. The pressure distribution is that of the NACA 63_1-012 section airfoil at zero angle of attack. In the experiments transition was artificially enforced at 20 percent of the chord for a Reynolds number of $5.4 \cdot 10^6$, zero lift conditions and a sweep angle of $\varphi = 45^\circ$. The skin friction coefficients as calculated with the present solution are shown in Fig. 2.

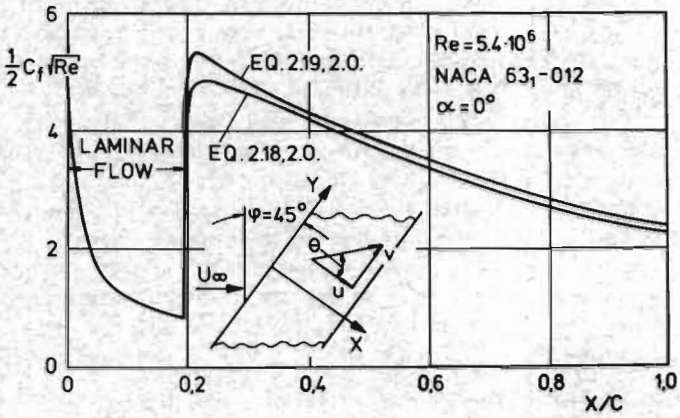

Fig. 2: Skin-friction coefficient calculated with the present solution for the measurements of Ref. [8.]

The integration was carried out by U. Müller of the Aerodynamische Institut. In the integration, a second-order solution (abbreviated 2.0 in Fig. 2 and subsequent Figs.) was used together with the closure relations equations(2.18) and(2.19). Both models yield almost the same results except for a short distance downstream from the point where transition was enforced.

In Fig. 3 the displacement thickness δ^* and momentum thickness θ as calculated with the

solution of Ref. [7] and the second-order solution presented in the foregoing sections are compared with the experimental data. The data shown in this Fig. correspond to those shown in Fig. 2.

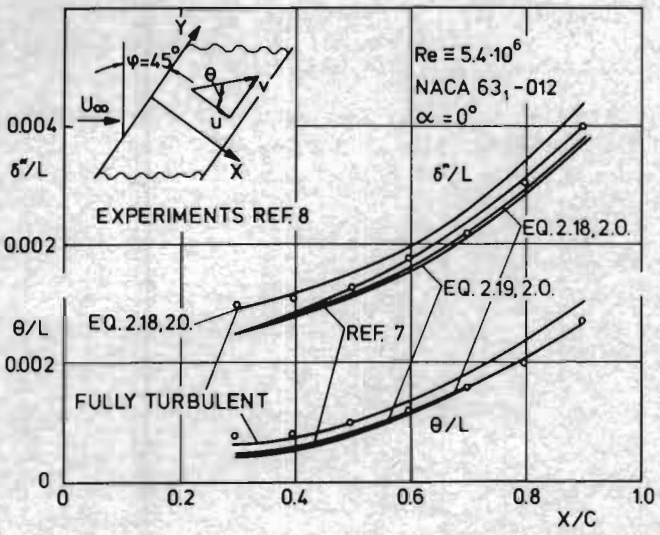

Fig. 3: Comparison of measured displacement and momentum thickness of Ref.[8] with predictions of Ref. [7] and of present second-order solution.

Deviations from the measured data can be noted immediately downstream from the transition point, but otherwise the accuracy of all three predictions is acceptable. The closure assumption used in Ref. [7] is almost identical to that of equation (2.21): Instead of the wall-shearing stress the local value is inserted in the van Driest damping factor but the pressure gradient is neglected. In both calculations the displacement thickness and the momentum thickness are evaluated for the x-component alone. The small deviations in the predictions are due to the differences in the closure assumptions and can also be noted in the velocity profiles (Fig. 4). At 50 percent chord the predictions obtained with the closure assumptions (2.18) and (2.19) show slightly fuller velocity profiles than those of Ref. [7]. Further downstream at x/c = o.6 all three predictions give virtually the same values; moreover, the agreement with the measurements is indeed good but not surprising since the pressure gradient is very small. The exchange coefficients are then at least approximately the same and the scalar assumption for ε is justified. On the other hand, the comparison in Fig. 4 does not confirm the validity of the three closure assumptions for three-dimensional but at most for two-dimensional boundary layers. Since the pressure gradient in the y-direction vanishes identically and is small in the x-direction the flow deviates only little from constant pressure conditions in the vicinity of 50 to 60 percent of the chord. Truely three-

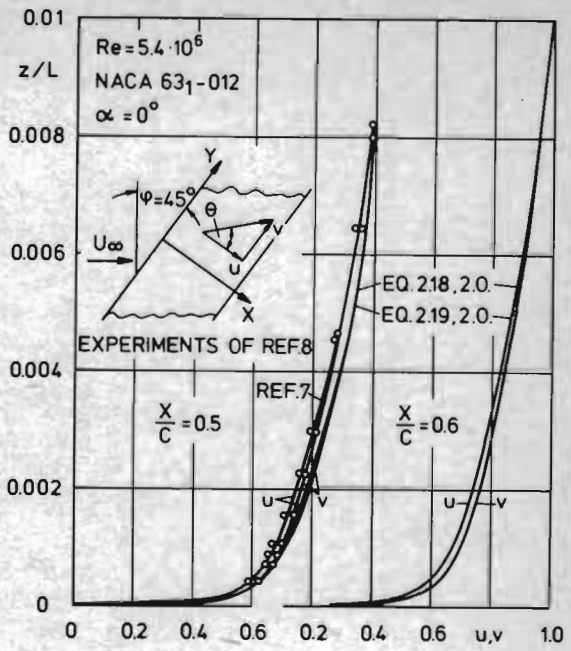

Fig. 4: Comparison of measured velocity profiles of Ref. [8] with predictions of Ref. [7] and of present second-order solution.

dimensional effects can therefore only be small as the projections of the local velocity vector on the plane of the surface of the wing are co-linear with that of the local turbulent shearing stress.

Large pressure gradients in the x-direction were enforced by van den Berg and Elsenaar in their experiment on an infinite swept wing [5]. Their flow conditions have been studied extensively with the present solution. The oncoming flow of the free-stream is incompressible with a Reynolds number of about $3.1 \cdot 10^6$. The sweep angle is 35^o and the pressure gradient is negative and large enough to lead to separation. W. Kordulla of the Aerodynamische Institut has carried out calculations in which all three closure assumptions, equations (2.18), (2.19), and (2.21) were employed. Both, second- and fourth-order algorithms were used. Thereby the numerical accuracy of the predictions could be determined for each closure assumption.

The range of predictions of the present solution is shown for the shearing stress in the upper part of Fig. 5. Although the agreement is fair downstream from the leading edge of the wing, the predictions fail near separation because of the scalar-assumptions introduced in the exchange coefficients. The details of the calculation are shown in the middle of Fig. 5. It is seen that the inclusion of the pressure gradient in the closure assumption (2.21) gives better agreement than equations (2.18) and (2.19) which are based on the wall shearing stress alone. It is of importance to point to purely numerical errors. Each calculation was carried out with second-order (2.0)

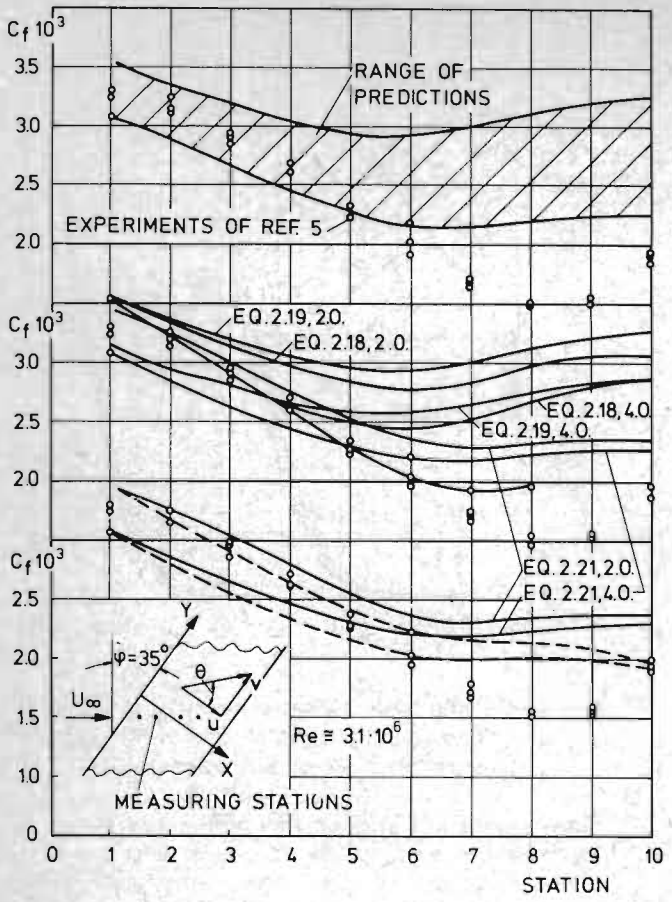

Fig. 5: Comparison of measured skin-friction coefficients with predictions of present second- and fourth-order solution. The curve which ends at point 8 is the prediction of Ref. [10]. The dashed lines give the skin-friction for δ^* based on the u-component of the velocity.

and fourth-order (4.0) truncation errors and substantial differences can be noted. These results should make clear that great care must be exercised in the numerical integration of the boundary-layer equations for turbulent flows. The curve which ends at measuring station 8 represents the prediction of Ref. [10]. These values were obtained after the law of the wall had been modified [10] and adjusted to three-dimensional flows.

In the lower part of Fig. 5 the predictions obtained with the closure assumption (2.21) are replotted for the second- and fourth-order solution. The solid line gives the shearing stress for the case when equation (2.21) is based on a displacement thickness evaluated for both velocity components. The dashed line gives the skin-friction coefficient for a displacement thickness based on the u-component of the velocity alone. Although there is agreement with the experimental data for the second-order solution, there is no justification of adopting the displacement thickness of the u-component for three-dimensional flows. The difference caused by the two assumptions just mentioned is substantial and does not support the simplifying assumptions of Ref. [6]. As the computational effort for the evaluation of the displacement thickness of the three-dimensional boundary layer is not much larger than for the two-dimensional one, δ^* should not be evaluated from the u-component alone.

The flow deflection as measured in the experiment of Ref. [5] and calculated by the present solution is shown in Fig. 6. Ag ain the assumption of

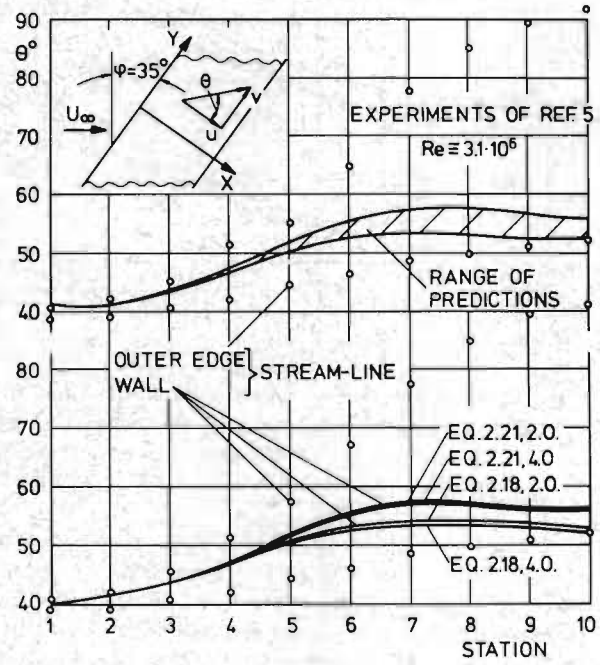

Fig. 6: Calculated and measured (Ref. [5]) flow deflection. Predictions are of present solution with second- and fourth-order accuracy.

colinearity between local shearing stress and the projection of the velocity vector is found to be invalid.

A comparison of calculated and measured velocity profiles is given in Fig. 7. For the measuring station 4 all six predictions fall almost together and are in acceptable agreement with the experiment. It is seen that the difference between second- and fourth-order solution is more pronounced in the shearing stress than in the velocity profiles. Near separation the predicted exchange of momentum is seen to be much too large for the x-direction. This is also indicated in Fig. 8 where for the two measuring stations the effective viscosities are plotted versus the coordinate normal to the wall. Despite the large deviations of equation (2.21) from (2.18) and (2.19) the corresponding differences in the velocity profiles are

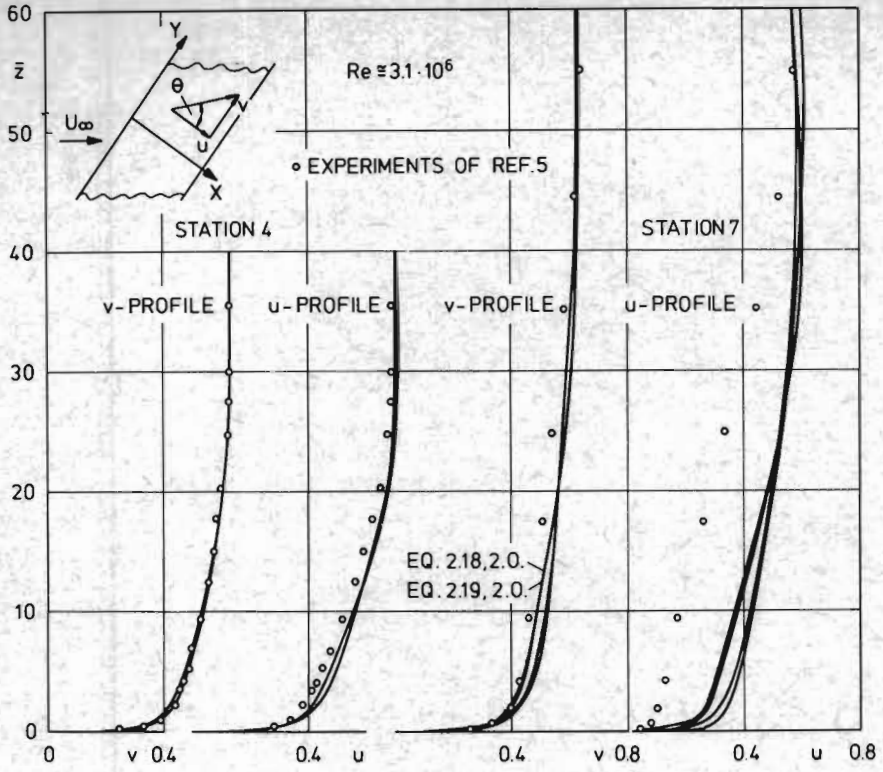

Fig. 7: Measured and calculated velocity profiles. Measurements are of Ref. [5]. Predictions of the present investigation.

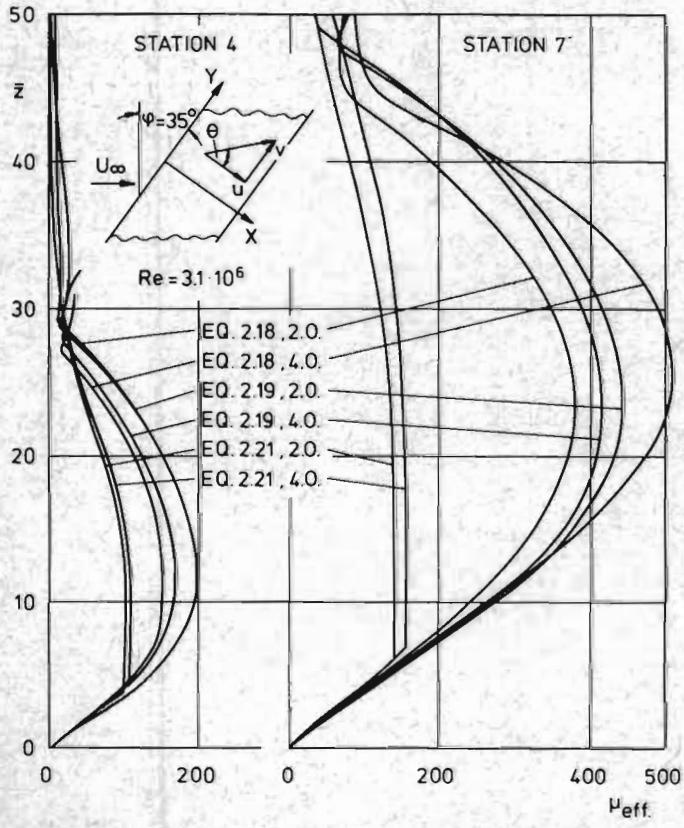

Fig. 8: Evaluation of closure assumptions for the velocity profiles shown in Fig. 7.

small. For more accurate predictions it is therefore necessary to investigate the closure assumptions for three-dimensional flows anew and construct more adequate formulations for the outer part of the boundary layer. Therein the vector characteristics of the exchange coefficients must be taken into account.

5. Conclusions

Several compressible laminar and incompressible turbulent boundary layers over infinite swept wings have been investigated. The boundary-layer equations were integrated with second and fourth-order accuracy. For turbulent flows three closure assumptions were included in comparison calculations. The results show that incompressible as well as compressible laminar three-dimensional boundary layers on wings can be predicted without difficulty. The restriction to infinite aspect ratio in the present investigation is of little importance. Boundary layers on wings with finite aspect ratio can be predicted with the same accuracy including large suction and blowing rates.

For turbulent flows it is shown that all three closure assumptions used in the present analysis fail near separation. The main reason for this failure is that in the outer part of the boundary layer the predicted momentum exchange is much too large and that the assumption of co-linearity between local shearing stress and the projection of the velocity vector on the plane of the surface of the wing is invalid. Models which are based on the displacement thickness of the boundary layer show a noticeable deviation if δ^* is evaluated with one velocity component only (two-dimensional approximation).

Finally it is noted that substantial errors in the predictions may result from the discretization

process. These errors may invalidate or considerably falsify the turbulence model adopted.

References

1. Goodmanson, L.T., and Gratzer, L.B., Recent Advances in Aerodynamics for Transport Aircraft. Part II. Astronautics and Aeronautics, January 1974.

2. Smith, P.D., An Integral Prediction Method for Three-Dimensional Compressible Turbulent Boundary Layers. Aeronautical Research Council R. and M. No. 3739. London. Her Majesty's Stationary Office 1974.

3. Cebeci, T., Attachment-Line Flow on an Infinite Swept Wing. AIAA J. Vol. 12, No. 2, pp. 242-245, February 1974.

4. East, L.F., Measurements of the Three-Dimensional Incompressible Turbulent Boundary Layer Induced on the Surface of a Slender Delta Wing by Leading Edge Vortex. RAE TR 7341, January 1974.

5. Van den Berg, B., and Elsenaar, A., Measurements in a Three-Dimensional Incompressible Turbulent Boundary Layer in an Adverse Pressure Gradient Under Infinite Swept Wing Conditions. NLR TR 12092 U, 1972.

6. Fannelop, T.K., and Humphreys, D.A., A Simple Finite-Difference Method for Solving the Three-Dimensional Turbulent Boundary-Layer Equations. AIAA Paper 74-13, AIAA 12th Aerospace Sciences Meeting, Washington D.C. January 30 - February 1, 1974.

7. Adams, J.C., Jr., Numerical Calculation of the Subsonic and Transonic Turbulent Boundary Layer on an Infinite Yawed Airfoil. AEDC-TR-73-112, July 1973.

8. Altman, J.M., and Hayter, N.F., A Comparison of the Turbulent Boundary-Layer Growth on an Unswept and a Swept Wing. NACA TN 2500, September 1951.

9. East, L.F., A Prediction of the Law of the Wall in Compressible Threedimensional Turbulent Boundary Layers. RAE TR 72178, November 1972.

10. Van den Berg, B., The Law of the Wall in Two- and Three-Dimensional Turbulent Boundary Layers. NLR TR 72111 U, 1973.

11. Krause, E., Hirschel, E.H., and Kordulla, W., Fourth Order "Mehrstellen"-Integration for Three-Dimensional Turbulent Boundary Layers Proceedings AIAA Computational Fluid Dynamics Conference Palm Springs, California, July 19-20, 1973.

12. Michel, R., Cousteix, J., Quémard, C., Application d'un schéma amélioré de longueur de mélange à l'étude des couches limités turbulentes tridimensionnelles. AGARD Meeting on Turbulent Shear Flows, London, 1971.

13. Pletcher, R.H., On a Finite Difference Solution for the Constant Property Turbulent Boundary Layer. AIAA Journal, Vol. 7, No. 2, Febr. 1969, pp. 305-311.

14. Hirschel, E.H., The Influence of the Free-Stream Reynolds Number on Transition in the Boundary Layer on an Infinite Swept Wing. Fluid-Motion-Problems in Wind Tunnel Design, AGARD-Report No. 602, 1973, pp. 1-1 - 1-11.

15. Krause, E., Numerical Solution of the Boundary Layer Equations. AIAA Journal, Vol. 5, No. 7, 1967, pp. 1231-1237.

16. Krause, E., Numerical Treatment of Boundary-Layer Problems. AGARD Lecture Series No. 64 on Advances in Numerical Fluid Dynamics, March 1973.

17. Keller, H.B., Cebeci, T., Accurate Numerical Methods for Boundary Layer Flows. Two Dimensional Laminar Flows, Proceedings of the Second International Conference on Numerical Methods in Fluid Dynamics, Lecture Notes in Physics, Vol. 8, 1971.

18. Krause, E., Mehrstellenverfahren zur Integration der Grenzschichtgleichungen, DLR-Mitt. 71-13, 1971, S. 109-138.

19. Krause, E., Comment on Solution of a Three-Dimensional Boundary-Layer Flow with Separation, AIAA Journal, Vol. 7, p. 575.

20. Beasley, J.A., Calculation of the Laminar Boundary Layer and the Prediction of Transition on a Sheared Wing. Fluid-Motion-Problems in Wind Tunnel Design, AGARD-Report No. 602, 1973, pp. 1-1 - 1-11.

21. Krause, E., Hirschel, E.H., Bothmann, Th., Differenzenformeln zur Berechnung dreidimensionaler Grenzschichten. DLR FB 69-66, 1969.